AMERICAN SOCIETY FOR MICROBIOLOGY | Molecular and Cellular Biology®

RESEARCH ARTICLE

# Long Noncoding RNA *GAS5* Inhibits Osteogenic Differentiation through MicroRNA 382-3p/*TAF1* Signaling

**Yuxin Song,[a,c] Hui Zhang,[a] Zhengdong Song,[a] Yang Yang,[a] Suifeng Zhang,[a] Wenji Wang,[a] Shanyong Zhang[b]**

[a]First School of Clinical Medicine of Lanzhou University, Department of Orthopedics, First Hospital of Lanzhou University, Lanzhou, Gansu, China
[b]Department of Oral Surgery, Ninth People's Hospital, College of Stomatology, Shanghai Jiao Tong University School of Medicine, Shanghai, China
[c]Department of Orthopedics, Gansu Provincial Hospital, Lanzhou, Gansu, China

**ABSTRACT** Long noncoding RNAs (lncRNAs) have been confirmed as important regulators during osteogenic differentiation. Previous research has disclosed that growth arrest-specific transcript 5 (*GAS5*) can promote osteogenic differentiation of human bone marrow mesenchymal stem cells (hBMSCs), but the underlying regulatory mechanism of *GAS5* during the osteogenic differentiation of hBMSCs is unclear. Osteogenic differentiation was induced in hBMSCs by using osteogenic medium (OM). Gene expression was assessed by quantitative real-time PCR (RT-qPCR) or Western blot assays as needed. Alkaline phosphatase (ALP) activity, ALP staining, and alizarin red S (ARS) staining assays were performed to evaluate the impact of *GAS5*, microRNA 382-3p (miR-382-3p), and TATA box binding protein-associated factor 1 (*TAF1*) on osteogenic differentiation *in vitro*. The interaction among *GAS5*, miR-382-3p, and *TAF1* was determined by RNA immunoprecipitation (RIP), chromatin immunoprecipitation (ChIP), and luciferase reporter assays. Expression of *GAS5* (transcript variant 2) was downregulated during the osteogenic differentiation of hBMSCs, and its overexpression retarded the osteogenic differentiation of hBMSCs. *GAS5* inhibited miR-382-3p by targeting RNA-directed microRNA degradation (TDMD). miR-382-3p downregulation partially offset the promoted osteogenic differentiation of hBMSCs upon *GAS5* silencing. *TAF1* negatively modulated osteogenic differentiation, and it activated *GAS5* transcription so as to form a positive *GAS5*-miR-382-3p-*TAF1* feedback loop in hBMSCs. This research was the first to reveal that the *GAS5*-miR-382-3p-*TAF1* feedback loop inhibited the osteogenic differentiation of hBMSCs, which provided new clues for exploring the mechanism of osteogenic differentiation and disclosed the potential of *GAS5* as a promising target during osteogenic differentiation.

**KEYWORDS** *GAS5*, miR-382-3p, *TAF1*, osteogenic differentiation

It is widely acknowledged that bones are pivotal to body protection, supporting, and shaping. In addition, bones are indispensable for vertebrates to move. The cellular components of bones include osteoclasts, osteoblasts, osteocytes, and osteogenic precursor cells (1). Moreover, the regeneration ability of bones is closely associated with skeletal development, bone injury, and continuous remodeling (2). During bone regeneration for the repair of injured parts, three major phases are involved, inflammation, formation of new bones, and bone remodeling (3). Human bone mesenchymal stem cells (hBMSCs) feature the ability to differentiate into nerve cells, chondrocytes, osteoblasts, or myocardial cells *in vitro*, which makes hBMSCs a perfect graft in bone tissue engineering (4). Notably, osteogenic differentiation plays a critical role in the maintenance of bone homeostasis (5). Therefore, it is of great significance to explore the mechanism underlying the osteogenic differentiation of hBMSCs.

Mounting evidence has validated that osteogenic differentiation of hBMSCs involves multiple factors, including long noncoding RNAs (lncRNAs) (6), the RNA molecules with a



Address correspondence to Wenji Wang, ldyyjzwwj@163.com, or Shanyong Zhang, qiushan03396629@163.com.

The authors declare no conflict of interest.

**Received** 12 October 2020
**Returned for modification** 25 October 2020
**Accepted** 3 December 2021
**Accepted manuscript posted online** 13 December 2021
**Published** 17 February 2022

length of over 200 nucleotides (nt) and without protein-coding capacities (7). For example, lncRNA *DANCR* regulates the proliferation and osteogenic differentiation of hBMSCs via the p38 MAPK pathway (8). lncRNA *BDNF-AS* modulates the osteogenic differentiation of BMSCs (9). lncRNA *MEG3* inhibits the osteogenic differentiation of BMSCs from postmenopausal osteoporosis by targeting miR-133a-3p (10). Growth arrest-specific transcript 5 (*GAS5*) is suggested to exert crucial functions in biological proliferation and differentiation (11–13). According to one previous study, *GAS5* promoted the osteogenic differentiation of human periodontal ligament stem cells by regulating the *GDF5* and p38/JNK signaling pathway (14). Another study has also disclosed that *GAS5* is upregulated in BMSCs. In addition, it can promote the osteogenic differentiation of BMSCs by regulating the miR-135a-5p/FOXO1 pathway (15). However, the mechanism of *GAS5* in regulating the osteogenic differentiation of hBMSCs still needs further exploration.

It is known that different transcript variants of lncRNAs may present different expression patterns in various human diseases (16, 17). Interestingly, our preliminary experiments discovered that *GAS5* had 15 transcript variants. Although several variants were upregulated during the osteogenic differentiation of hBMSCs, the *GAS5* transcript variant 2 was downregulated. Therefore, this study focused on *GAS5* with the aim of uncovering whether *GAS5* (transcript variant 2) may play a significant role during osteogenic differentiation. This study might provide some innovative ideas for research on the mechanism of *GAS5* and unveil its potential as a target during osteogenic differentiation.

## RESULTS

***GAS5* transcript variant 2 was downregulated during the osteogenic induction of hBMSCs.** First, we simulated the osteogenic differentiation of hBMSCs by incubating hBMSCs in osteogenic differentiation medium (OM), and growth culture medium was used as internal control. To examine the osteogenic differentiation of hBMSCs, we detected the expression levels of three key osteogenic genes (*RUNX2*, *OSX*, and *ALPL*) in hBMSCs at days 0, 3, 7, 14, and 21 after incubation. As a result, *RUNX2*, *OSX*, and *ALPL* expression was observed to be gradually elevated in hBMSCs incubated in OM but not in growth medium (GM) (Fig. 1A to C), suggesting a successful induction of osteogenic differentiation in hBMSCs by using OM.

Next, we tried to figure out the role of *GAS5* during osteogenic differentiation. According to the data collected from the UCSC database, there were 15 transcript variants of *GAS5* in total. After that, to figure out which transcript variants of *GAS5* could actually participate in the osteogenic differentiation of hBMSCs, we detected the expression of all 15 transcript variants (T1 to T15) in hBMSCs at day 0 and day 7 during osteogenic differentiation. Interestingly, we found that the expression of transcript variants 6, 11, and 13 was significantly upregulated, whereas the expression of transcript variant 2 was obviously downregulated in hBMSCs at day 7 after the incubation in OM (Fig. 1D). According to one previous study, *GAS5* is upregulated during osteogenic differentiation and can promote the osteogenic differentiation of hBMSCs (15). However, our study discovered that transcription variant 2 of *GAS5* was downregulated in hBMSCs during osteogenic differentiation. Also, we confirmed through quantitative real-time PCR (RT-qPCR) assay that the expression of transcription variant 2 of *GAS5* was gradually decreased during the osteogenic differentiation of hBMSCs (Fig. 1E). Those data indicated that transcript variant 2 of *GAS5* potentially played a suppressive role during the osteogenic induction of hBMSCs. Therefore, transcript variant 2 of *GAS5* was referred to as *GAS5* for the following assays.

***GAS5* suppressed osteogenic differentiation of hBMSCs.** Subsequently, to investigate the role of *GAS5* during the osteogenic differentiation of hBMSCs, we constructed plasmids for *GAS5* silencing (sh-*GAS5*-1/2/3) and overexpression (pcDNA3.1/*GAS5*). After that, an RT-qPCR assay was adopted to detect the overexpression efficiency and interference efficiency of *GAS5* in hBMSCs (Fig. 2A). As the interference efficiency of sh-*GAS5*-1 and sh-*GAS5*-2 was better than that of sh-*GAS5*-3, they were kept for further experiments. Then, the expression of *RUNX2*, *OSX*, and *ALPL* was measured after the osteogenic induction at day 7 in transfected hBMSCs. The results manifested

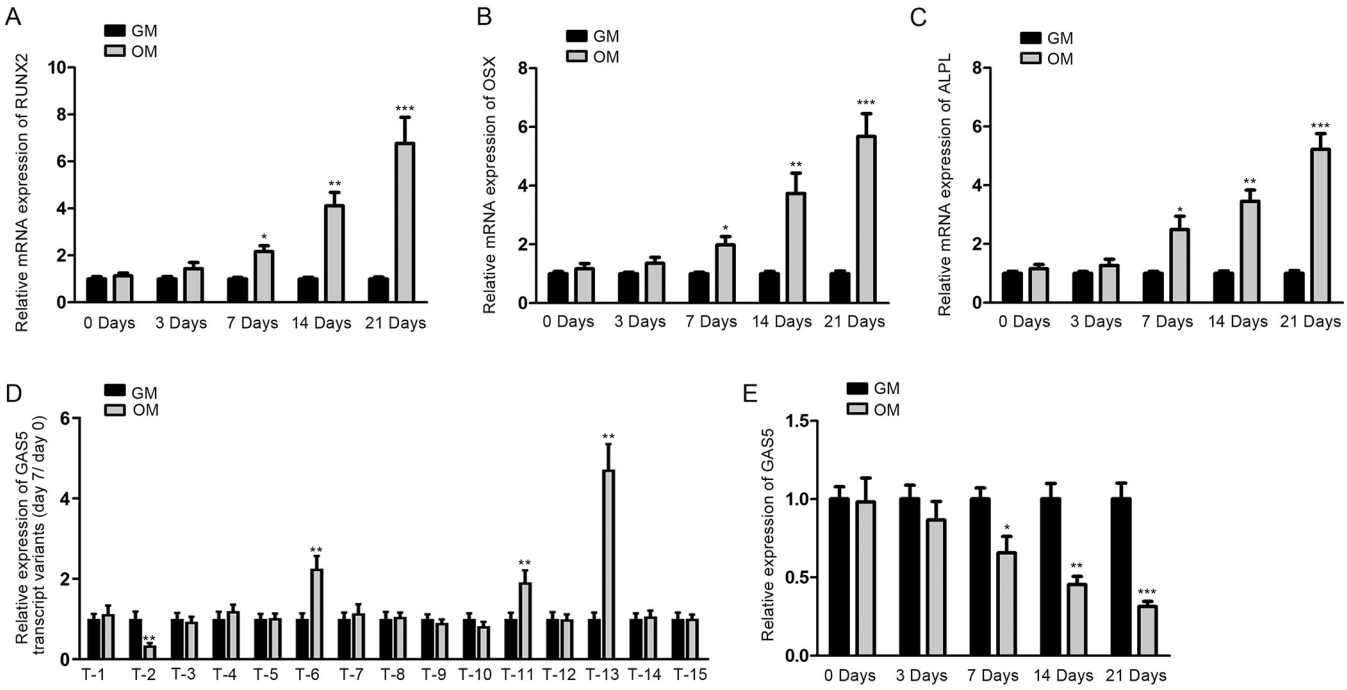


**FIG 1** *GAS5* transcript variant 2 was downregulated during the osteogenic induction of hBMSCs. (A to C) Relative mRNA levels of *RUNX2*, *OSX*, and *ALPL* were examined by RT-qPCR assay in hBMSCs after the incubation for 0, 3, 7, 14, and 21 days in osteogenic medium (OM) relative to growth medium (GM). (D) RT-qPCR assay was conducted to detect the expression levels of 15 transcript variants of *GAS5* at day 7 normalized to day 0 of incubation in OM relative to GM. (E) The expression of *GAS5* in hBMSCs during osteogenic differentiation in OM relative to GM at days 0, 3, 7, 14, and 21 was detected by RT-qPCR assay. *, $P < 0.05$; **, $P < 0.01$; ***, $P < 0.001$.

that *RUNX2*, *OSX*, and *ALPL* mRNA levels were upregulated upon *GAS5* silencing, while they were downregulated after *GAS5* overexpression (Fig. 2B). According to the result of Western blot assay, *GAS5* silencing could lead to elevated protein levels of *RUNX2* and *OSX*, while *GAS5* overexpression led to an opposite result (Fig. 2C). Also, to further identify the effects of *GAS5* on osteogenic differentiation, alkaline phosphatase (ALP) activity, alizarin red S (ARS) staining, and ALP staining assays were carried out. It was shown that *GAS5* knockdown not only increased ALP activity but also promoted the formation of mineralized bone matrix, whereas *GAS5* overexpression dramatically inhibited ALP activity and mineralized bone matrix formation (Fig. 2D and E). Taken together, *GAS5* inhibited the osteogenic differentiation of hBMSCs.

***GAS5* could inhibit miR-382-3p through the targeting RNA-directed microRNA degradation mechanism.** Our next step was to figure out how *GAS5* may function to inhibit the osteogenic differentiation of hBMSCs. The interaction between microRNA (miRNAs) and lncRNAs has been substantially reported in osteogenesis before (15, 18), so we speculated that *GAS5* may interact with certain miRNAs to exert its function during hBMSCs osteogenic differentiation. First, the starBase v2.0 website (http://starbase.sysu.edu.cn/index.php) was utilized to forecast potential miRNAs of *GAS5*. As a result, miR-382-3p, miR-205-5p, miR-223-3p, miR-455-5p, and miR-433-3p were selected as candidates (Fig. 3A). According to the result of the RT-qPCR assay, the expression of miR-382-3p was the most upregulated miRNA in hBMSCs transfected with sh-*GAS5*-1/2 (Fig. 3B). Moreover, a former study has suggested that miR-382-3p can promote osteogenic differentiation (19). Consistently, we further confirmed that miR-382-3p level was increased during osteogenic differentiation by comparing the expression level of it in the GM and OM (Fig. 3C). Based on those data, we speculated that *GAS5* might exert its function through interacting with miR-382-3p.

One previous research has discovered that miRNAs can be inhibited through the targeting RNA-directed microRNA degradation (TDMD) model (20), so we proceeded to explore whether *GAS5* inhibited miR-382-3p through this mechanism. An RNA

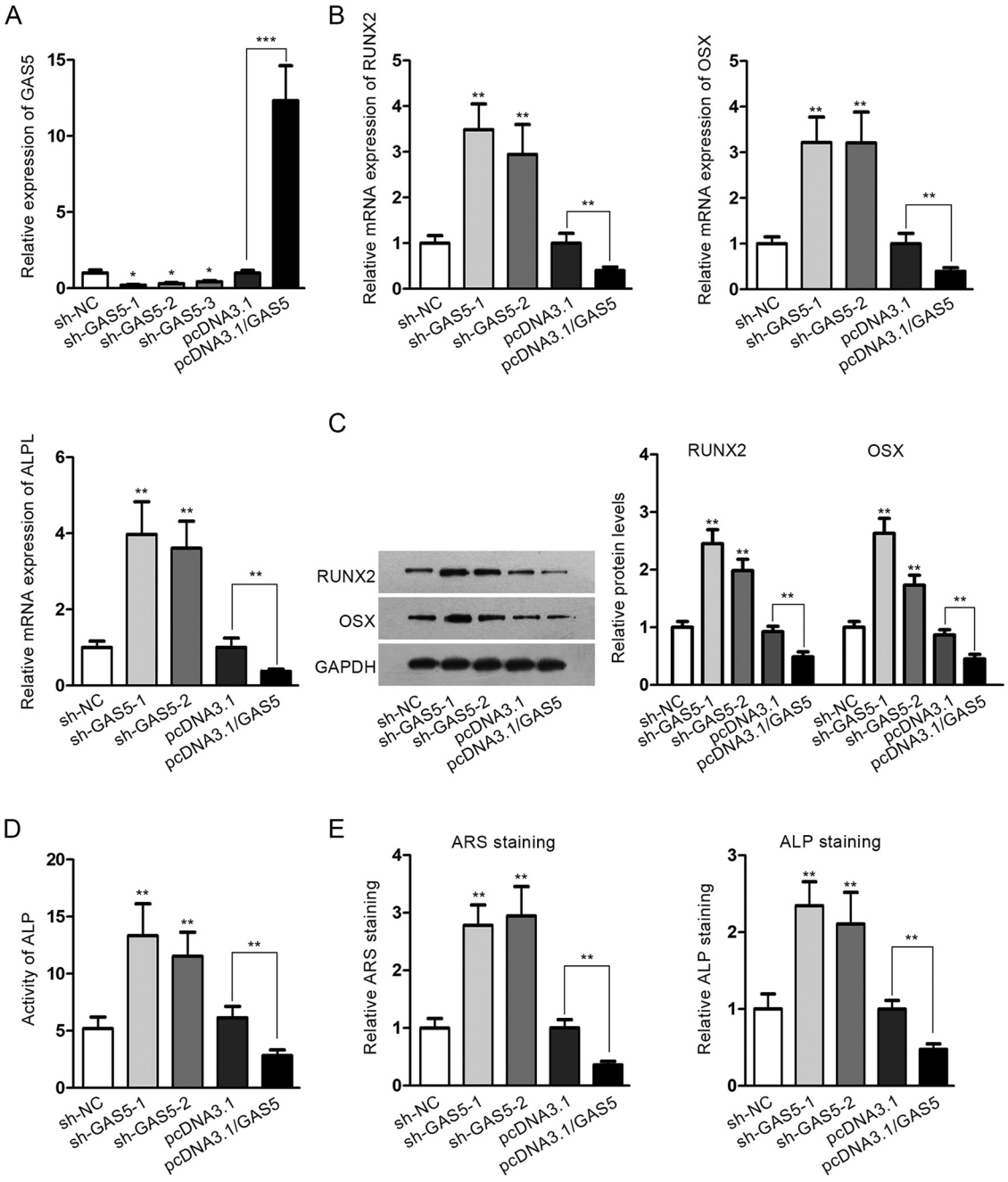


**FIG 2** *GAS5* suppressed osteogenic differentiation of hBMSCs. (A) Transfection efficiency of three *GAS5*-targeting short hairpin RNAs (shRNAs) (sh-*GAS5*-1/2/3) and pcDNA3.1/*GAS5* in hBMSCs was tested by RT-qPCR assay. (B) *RUNX2*, *OSX*, and *ALPL* mRNA levels in transfected hBMSCs after osteogenic transduction were detected by RT-qPCR assay. (C) *RUNX2* and *OSX* protein levels in transfected hBMSCs after osteogenic transduction were detected by Western blot assay. (D) ALP activity assay was conducted to measure ALP activity upon the overexpression or knockdown of *GAS5* in hBMSCs after osteogenic transduction. (E) ARS and ALP staining was carried out in hBMSCs after osteogenic induction for 7 days to examine ALP activity and mineralized bone matrix formation upon the ectopic *GAS5* expression. *, $P < 0.05$; **, $P < 0.01$; ***, $P < 0.001$.

pulldown assay was conducted, and the result demonstrated that miR-382-3p was enriched in Bio-*GAS5*-wild-type (WT) group, while no obvious change was found in Bio-NC and Bio-*GAS5*-Mut groups (Fig. 3D), which preliminarily proved our speculation. Next, by conducting an RT-qPCR assay, we confirmed that the knockdown of *GAS5* elevated the expression level of miR-382-3p, while the overexpression of *GAS5* reduced miR-382-3p expression. We also observed that the overexpression of *GAS5* (Mut) (with mutant miR-382-3p site) could not decrease the miR-382-3p level in hBMSCs (Fig. 3E,

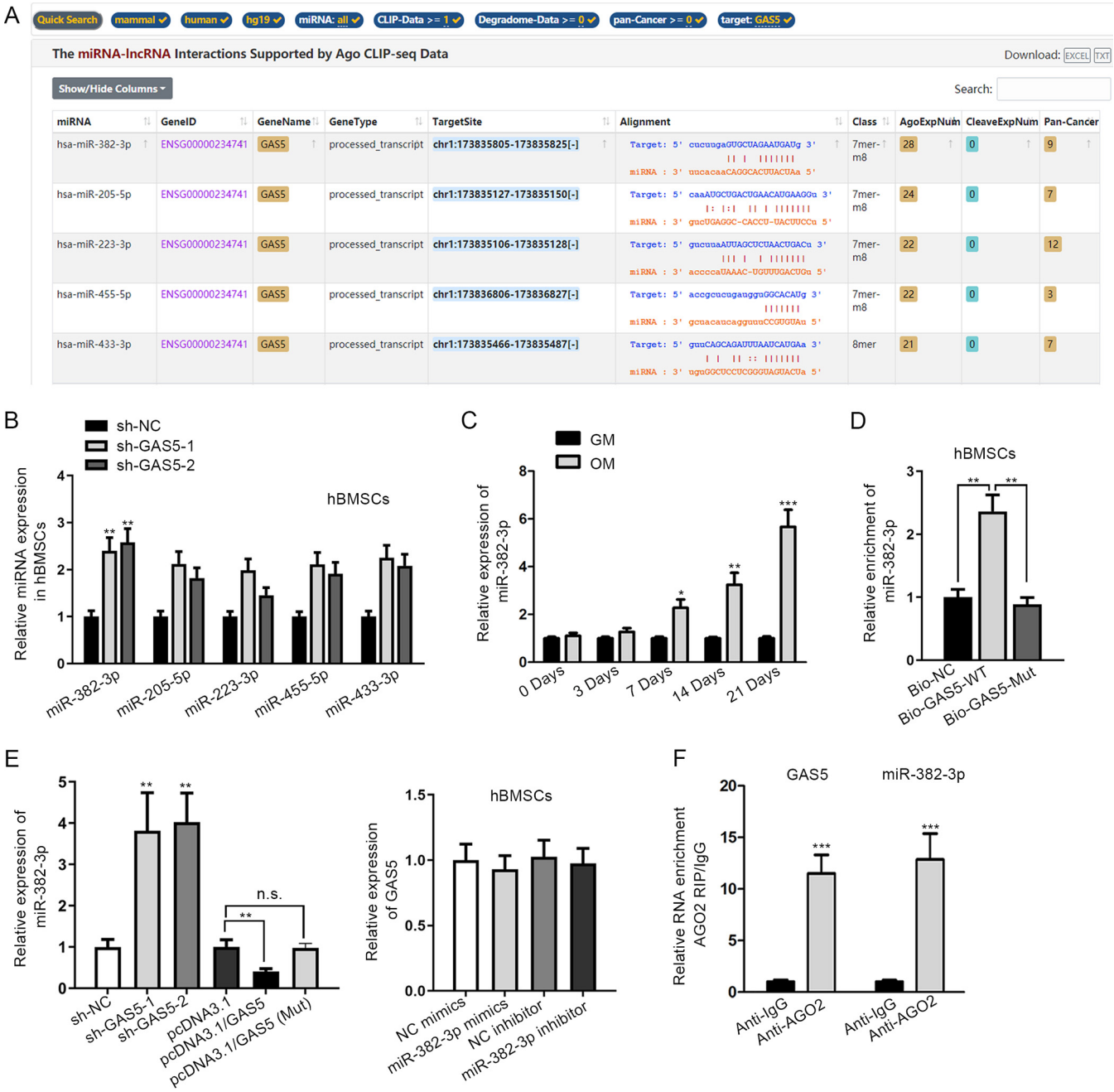


**FIG 3** *GAS5* could inhibit miR-382-3p through TDMD mechanism. (A) Potential miRNAs which could bind to *GAS5* were predicted by using starBasev2.0. (B) RT-qPCR assay was used to detect the expression levels of 5 predicted miRNAs in hBMSCs under *GAS5* silencing and osteogenic induction. (C) Expression of miR-382-3p in hBMSCs after 0, 3, 7, 14, and 21 days of incubation in OM or GM was detected by RT-qPCR assay. (D) RNA pulldown assay was conducted to confirm the physical interaction between *GAS5* and miR-382-3p in hBMSCs at the predicted sites. (E) Expression of miR-382-3p and *GAS5* was detected by RT-qPCR assay in hBMSCs under different transfection conditions. (F) RIP assay was conducted to confirm the association of *GAS5* with miR-382-3p. n.s., no significance; *, $P < 0.05$; **, $P < 0.01$; ***, $P < 0.001$.

left). Additionally, we found that the transfection of miR-382-3p mimics or inhibitor did not affect the expression of *GAS5* in hBMSCs (Fig. 3E, right). After that, an RIP assay was conducted, and it was verified that both *GAS5* and miR-382-3p were enriched in anti-AGO2 groups rather than in anti-IgG groups (Fig. 3F), suggesting their coexistence in RNA-induced silencing complexes (RISCs). Altogether, *GAS5* could inhibit miR-382-3p through the TDMD mechanism in hBMSCs.

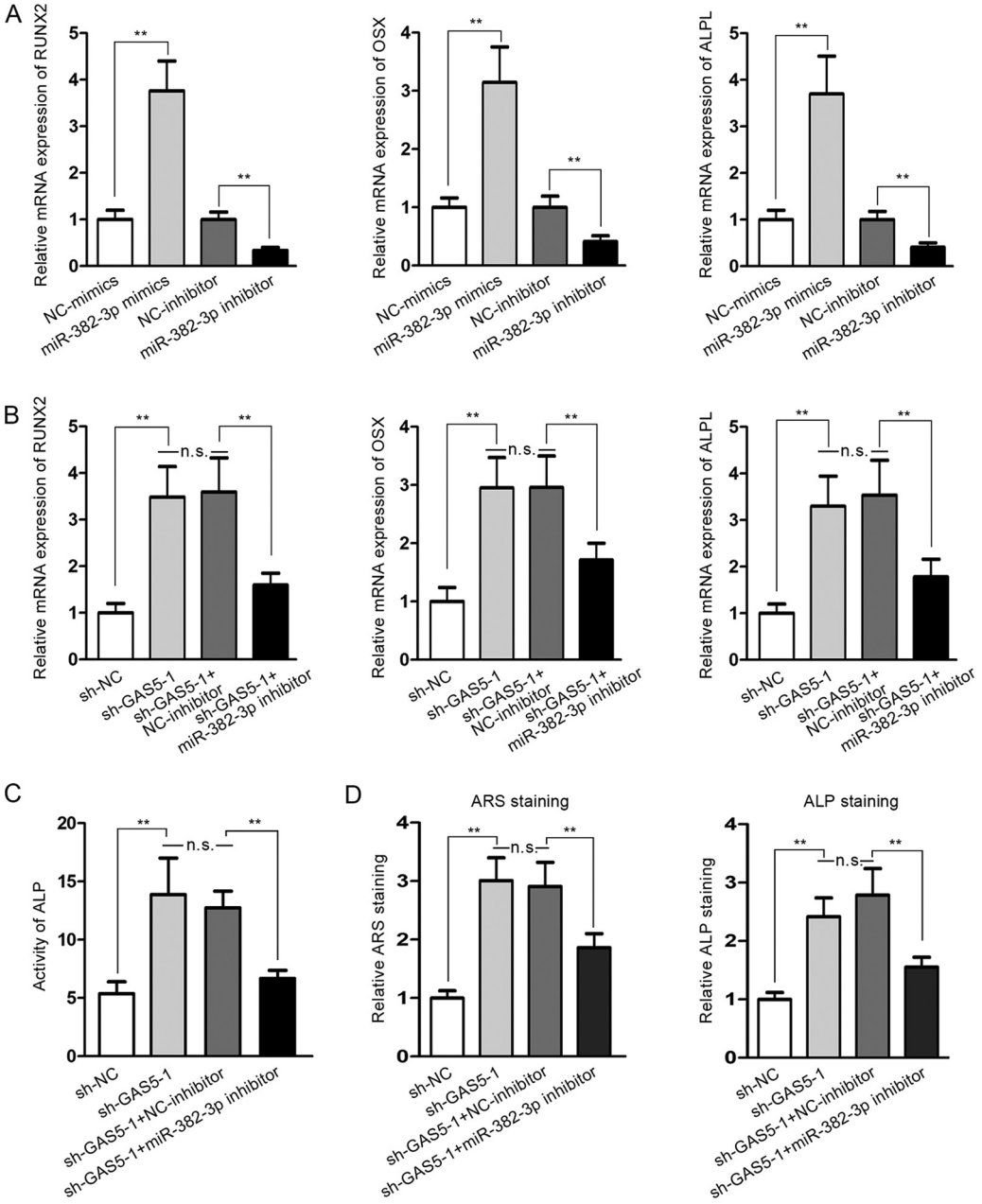


**FIG 4** *GAS5* negatively regulated miR-382-3p during osteogenic induction. (A) *RUNX2*, *OSX*, and *ALPL* mRNA levels in hBMSCs under different transfection conditions were measured by RT-qPCR assay after 7 days of osteogenic induction. (B) *RUNX2*, *OSX*, and *ALPL* mRNA expression was determined by RT-qPCR assay in hBMSCs transfected with sh-NC, sh-*GAS5*-1, sh-*GAS5*-1 plus NC inhibitor and sh-*GAS5*-1+miR-382-3p inhibitor after osteogenic induction. (C) ALP activity assay was carried out 7 days after osteogenic transduction under different transfection conditions. (D) ARS and ALP staining assays were conducted 7 days after osteogenic transduction under different transfection conditions. n.s., no significance; **, $P < 0.01$.

***GAS5* negatively regulated miR-382-3p to inhibit osteogenic differentiation *in vitro*.** As miR-382-3p has been unveiled to enhance the osteogenic differentiation of cells (19), we also tried to validate the influence of miR-382-3p on the osteogenic differentiation of hBMSCs. According to the result of RT-qPCR assays, the expression levels of *RUNX2*, *OSX*, and *ALPL* were elevated by the transfection of miR-382-3p mimics, while they were declined again by inhibiting miR-382-3p expression (Fig. 4A). In addition, rescue assays were carried out to verify the function of the *GAS5*/miR-382-3p axis during the osteogenic differentiation of hBMSCs. As shown by the result of the RT-qPCR assay, it was observed that the cotransfection of miR-382-3p inhibitor partially

reversed the promoting impact on the *RUNX2*, *OSX*, and *ALPL* expression in hBMSCs caused by *GAS5* silencing after 7 days of osteogenic induction (Fig. 4B). Consistently, the increased ALP activity caused by *GAS5* silencing was partially rescued by miR-382-3p inhibition (Fig. 4C). Likewise, matrix mineralization and ALP staining that were enhanced by *GAS5* depletion were both partially recovered by the cotransfection of miR-382-3p inhibitor (Fig. 4D). To conclude, *GAS5* negatively regulated miR-382-3p to inhibit the osteogenic differentiation of hBMSCs *in vitro*.

***TAF1* was a target of the *GAS5*/miR-382-3p axis during osteogenic differentiation.** As mentioned above, we have verified that *GAS5* could bind to miR-382-3p. As it has been proven that lncRNAs can bind to miRNAs, thus upregulating the expression level of certain genes, we then tried to determine the downstream targets of miR-382-3p. Through starBase, *TAF1* was predicted to interact with miR-382-3p. Notably, *TAF1* has been reported to be involved in osteogenic differentiation (21). Then, we searched for the binding sites between *TAF1* and miR-382-3p on UCSC Genome Browser (http://genome.ucsc.edu/), and the results are presented in Fig. 5A. Then, the TAF1 3′ untranslated region (UTR) with wild-type or mutant miR-382-3p sites was used to generate TAF1-Wt/Mut luciferase reporters. The result of luciferase reporter assays indicated that the luciferase activity of cells transfected with *TAF1*-Wt was significantly reduced after the transfection of miR-382-3p mimics but elevated upon miR-382-3p silencing (Fig. 5B, left). Also, it was shown that the reduced luciferase activity caused by miR-382-3p overexpression was reversed by the overexpression of *GAS5* rather than *GAS5* (Mut) (Fig. 5B, right). Moreover, according to the result of Western blotting and RT-qPCR assays, it was verified that *TAF1* protein and mRNA levels were both decreased upon miR-382-3p overexpression and increased upon miR-382-3p silencing (Fig. 5C and D). Furthermore, we examined whether *GAS5* may compete with *TAF1* for miR-382-3p. As shown by Fig. 5E (left and middle), we found that *GAS5* knockdown elevated *TAF1* enrichment in anti-AGO2-precipitated compounds, whereas *GAS5* overexpression led to a notably opposite result. Moreover, it was found through RIP assay that *GAS5* (Mut) overexpression failed to alter the enrichment of *TAF1* in AGO2 RIP products, indicating that the miR-382-3p site was required for *GAS5* to interfere with the incorporation of *TAF1* into RISC. Moreover, it was found that miR-382-3p mimics led to an increase in the enrichment of *GAS5* and *TAF1* in AGO2 RIP products, whereas miR-382-3p inhibitor caused opposite outcomes (Fig. 5E, right), indicating that miR-382-3p was required for the incorporation of *GAS5* and *TAF1* into RISC. Considering those data, we confirmed that *GAS5* could bind to miR-382-3p, thus releasing *TAF1* from being targeted by miR-382-3p in hBMSCs.

Next, we decided to verify the influence of *TAF1* on the osteogenic differentiation of hBMSCs. By carrying out Western blotting and RT-qPCR assays, we confirmed that the silencing of *TAF1* elevated the expression levels of *RUNX2* and *OSX* proteins, whereas *TAF1* overexpression led to opposite results in hBMSCs (Fig. 5F). Consistently, ALP activity, ALP staining, as well as mineralized matrix nodules in hBMSCs, were all enhanced upon *TAF1* silencing while being reduced upon *TAF1* overexpression (Fig. 5G and H). Therefore, *TAF1* was a target of the *GAS5*/miR-382-3p axis in the osteogenic differentiation of hBMSCs.

***TAF1* formed a positive feedback loop with *GAS5*/miR-382-3p.** *TAF1* belongs to the TAFs family, participating in basal transcription by functioning as coactivators (22). Multiple transcription activators have been proven to activate lncRNAs in human diseases (23, 24), including in osteogenic differentiation (25). Therefore, we wondered whether *TAF1* may activate *GAS5* in turn. First, we obtained the promoter sequences of *GAS5* and screened it on the HumanTFBD website (http://bioinfo.life.hust.edu.cn/HumanTFDB/#!) ($Q < 0.01$, score $> 20$), and we found 2 potential *TAF1* binding sites on the *GAS5* promoter (Fig. 6A; Supplemental File 1). Then, the result of chromatin immunoprecipitation (ChIP) assay revealed the enrichment of *GAS5* promoter fragments with either site 1 or site 2 in *TAF1* binding complex, which confirmed the binding ability of *TAF1* to the *GAS5* promoter in hBMSCs (Fig. 6A). Also, results from the luciferase reporter assay demonstrated that the relative luciferase activity of *GAS5* promoter was inhibited by *TAF1* silencing (Fig. 6B). Also, it was certified that the expression of *GAS5* was dramatically decreased in hBMSCs upon

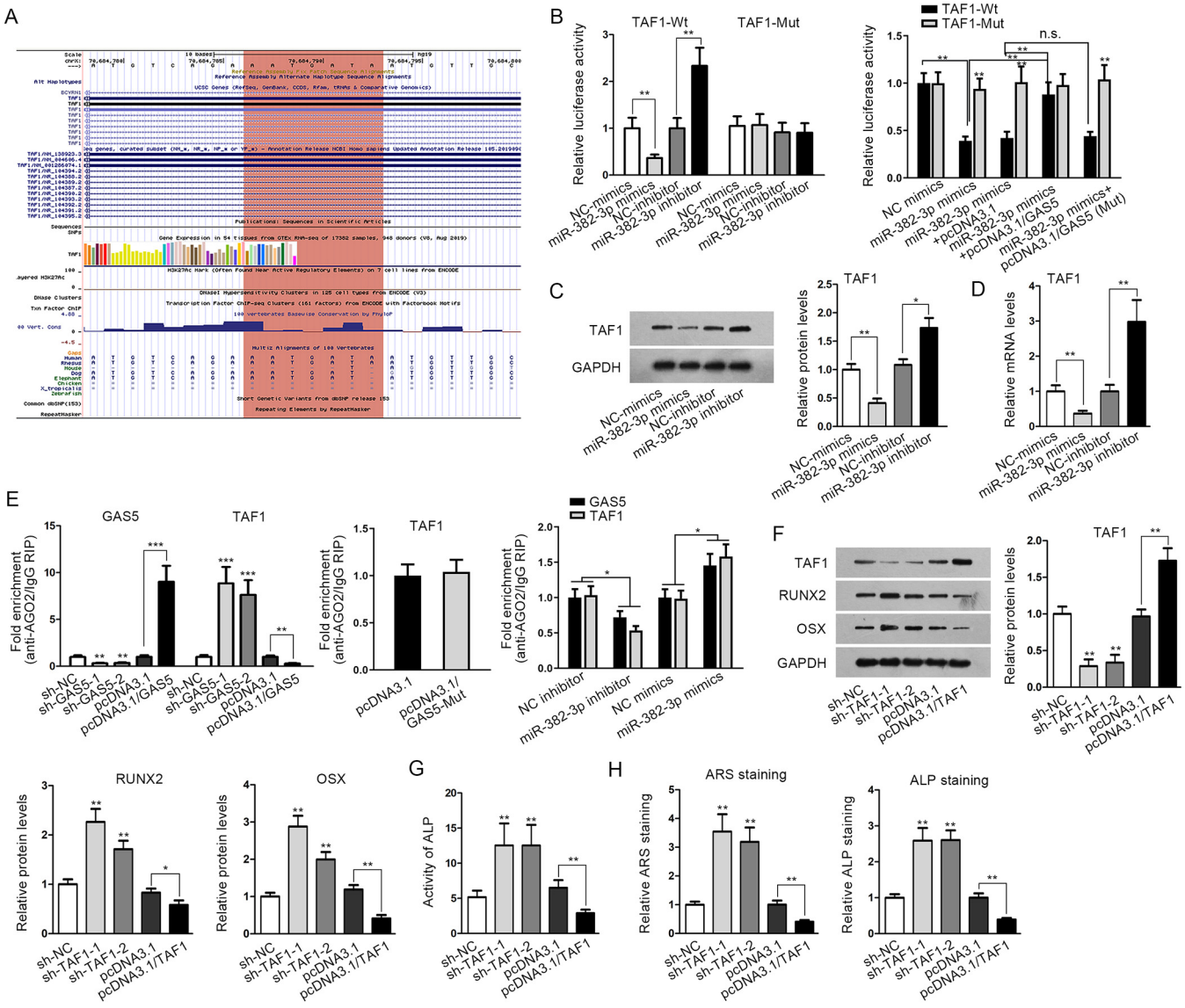


**FIG 5** *TAF1* was a target of the *GAS5*/miR-382-3p axis during osteogenic differentiation. (A) The putative binding sites between miR-382-3p and *TAF1* were predicted by starBasev2.0 and revealed in the UCSC Genome Browser. (B) Luciferase reporter assay was carried out to evaluate the luciferase activity of *TAF1*-Wt/Mut in hBMSCs transfected with miR-382-3p mimics/inhibitor relative to NC mimics/inhibitor (left) and the luciferase activity of *TAF1*-Wt/Mut in hBMSCs transfected with NC mimics, miR-382-3p mimics, miR-382-3p mimics plus pcDNA3.1, miR-382-3p mimics plus pcDNA3.1/*GAS5*, and miR-382-3p mimics plus pcDNA3.1/*GAS5* (Mut) (right). (C) *TAF1* protein levels in hBMSCs under different transfection conditions were assessed by Western blot assay. (D) *TAF1* mRNA level in hBMSCs under different transfection conditions was assessed by RT-qPCR assay. (E) RIP assay was conducted to detect the enrichment of *GAS5* and *TAF1* in AGO2 RIP product relative to IgG RIP product in hBMSCs transfected with sh-NC, sh-GAS5-1/2, pcDNA3.1, pcDNA3.1/GAS5, and pcDNA3.1/GAS5 (Mut) (left and middle) or with NC mimics/inhibitor and miR-382-3p mimics/inhibitor (right). (F) The protein levels of *TAF1*, *RUNX2*, and *OSX* were measured by Western blot assay in hBMSCs upon TAF1 knockdown or overexpression after osteogenic induction. (G) ALP activity assay was conducted in hBMSCs after osteogenic induction to examine the activity of ALP upon the knockdown or overexpression of *TAF1*. (H) ARS and ALP staining assays were carried out in hBMSCs after osteogenic induction to examine mineralized bone matrix formation upon the knockdown or overexpression of *TAF1*. n.s., no significance; *, $P < 0.05$; **, $P < 0.01$; ***, $P < 0.001$.

*TAF1* silencing (Fig. 6C). In order to further detect the effect of *TAF1* on *GAS5* transcription, expression of *GAS5* precursor RNA (*pre-GAS5*) was detected. After conducting the RT-qPCR assay, it was confirmed that the expression of *pre-GAS5* in hBMSCs was decreased by *TAF1* knockdown, while it was increased by *TAF1* overexpression in hBMSCs (Fig. 6D). Considering all the results above, it was concluded that *TAF1* activated *GAS5* transcription so that *GAS5*, miR-382-3p, and *TAF1* formed a positive regulatory feedback loop in hBMSCs to negatively regulate osteogenic differentiation (Fig. 6E).

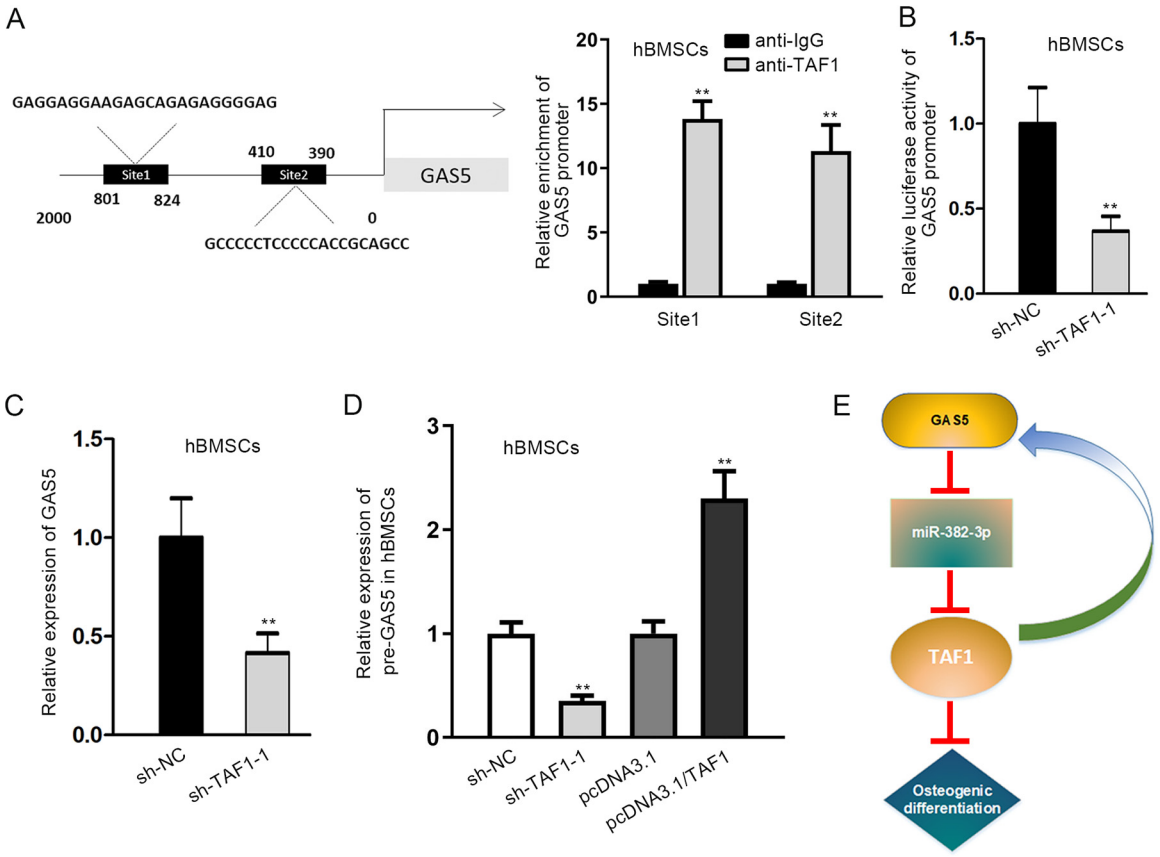


**FIG 6** *TAF1* formed a feedback loop with *GAS5*/miR-382-3p. (A, left) *TAF1* binding site on *GAS5* promoter was predicted by the HumanTFDB website (left). (A, right) The enrichment of *GAS5* promoter fragments with site 1 and site 2 in *TAF1* binding complex was measured by ChIP assay. (B) Luciferase activity of *GAS5* promoter in hBMSCs upon *TAF1* knockdown was evaluated by luciferase reporter assay. (C) *GAS5* expression upon *TAF1* silencing was tested by RT-qPCR assay. (D) Expression of *pre-GAS5* was detected by RT-qPCR assay in hBMSCs transfected with sh-*TAF1* and pcDNA3.1/*TAF1*. (E) Graphical abstract of the *GAS5*/miR-382-3p/*TAF1* feedback loop in osteogenic differentiation is presented. **, $P < 0.01$.

## DISCUSSION

It is known that hBMSCs can differentiate multiple types of cells, including osteoblasts (4). Importantly, osteogenic differentiation is a key function of hBMSCs which is closely associated with the formation and remodeling of bone (3, 5), suggesting that hBMSCs are crucial to bone damage repairing. Therefore, it is of great importance to explore the mechanism behind the osteogenic differentiation of hBMSCs.

Various lncRNAs have been characterized as important regulators in osteogenic differentiation. For example, long noncoding RNA *XIST* promotes osteoporosis through inhibiting bone marrow mesenchymal stem cell differentiation (26). *lnc-NTF3-5* promotes the osteogenic differentiation of maxillary sinus membrane stem cells via sponging miR-93-3p (27). lncRNA *OIP5-AS1* inhibits the osteoblast differentiation of valve interstitial cells via the miR-137/*TWIST11* axis (28). Several previous studies have disclosed that *GAS5* is upregulated during the osteogenic differentiation of human periodontal ligament stem cells and BMSCs. In addition, such a gene can promote osteogenic differentiation (29–31). However, increasing research has suggested that different transcript variants of lncRNAs can present different expression patterns and function differently in different human diseases. For example, the longest transcript of lncRNA, *ANRIL*, is upregulated in coronary arteries of coronary artery disease (CAD) patients (16); transcript variant 2 of *SCAMP1* can inhibit the progression of breast cancer (32). In cervical cancer cells, the transcript variant 7 of *SOX2OT* is highly expressed, whereas the level of variant 1 of *SOX2OT* is low (33). Herein, we obtained 15 transcript variants of *GAS5* from the UCSC Genome Browser and detected their expression in hBMSCs during

osteogenic differentiation. We confirmed that variants 6, 11, and 13 were upregulated during the osteogenic induction of hBMSCs, indicating those variants might be the target variants contributing to osteogenic differentiation as former studies have indicated. Interestingly, we first discovered that the transcript variant 2 of *GAS5* was downregulated in hBMSCs during osteogenic differentiation. Therefore, we speculated that *GAS5* variant 2 could present different expression patterns, as it was the longest variant with one more exon than the other 14 *GAS5* variants. Those data indicated that *GAS5* variant 2 might be negatively related to osteogenic differentiation. Furthermore, we confirmed that overexpressing *GAS5* could inhibit the osteogenic differentiation of hBMSCs. Referring to previous literature, interactions between lncRNAs and miRNAs in osteogenesis are widely reported. Herein, we predicted that miRNAs could potentially bind to *GAS5*, and we first discovered that miR-382-3p was negatively regulated by *GAS5* in hBMSCs. Formerly, it has been elucidated that miR-382-3p can enhance the osteogenic differentiation of adipose tissue-derived mesenchymal stem cells (19). Herein, we confirmed that the miR-382-3p level was elevated during osteogenic differentiation in hBMSCs, which was consistent with the former study suggesting that miR-382-3p was positively related to osteogenic differentiation.

Moreover, we explored how *GAS5* inhibited miR-382-3p expression. It has been reported that miRNA expression could be inhibited by TDMD (20). Herein, we confirmed that *GAS5* physically interacted with miR-382-3p at predicted sites and that *GAS5* could inhibit miR-382-3p activity and expression. Those data indicated that *GAS5* inhibited miR-382-3p via a TDMD mechanism.

Meanwhile, according to the AGO2-RIP assay, we found that *GAS5* and miR-382-3p coexisted in RISC as well. Although it was proved that *GAS5* was downregulated during osteogenic differentiation, it was possible that overexpressing *GAS5* in differentiated hBMSCs could increase the *GAS5* level. In addition, several works have reported that downregulated lncRNAs can serve as negative regulators for osteogenic differentiation by sponging miRNAs (34, 35). Consistently, our study was the first to confirm that *GAS5* could bind to miR-382-3p to inhibit hBMSC osteogenic differentiation.

Later, we found that *TAF1* was a putative target gene of miR-382-3p. Iwata et al. have discovered that *TAF1* is downregulated at the initial stage of osteogenic differentiation and can decrease *TAF1* expression, thus resulting in increased expression of *RUNX2* (21). Accordingly, our study was the first to reveal that *GAS5* competitively bound with miR-382-3p to prevent miR-382-3p from incorporating *TAF1* into RISC, thus inhibiting *TAF1* expression. Moreover, we confirmed that *TAF1* negatively regulated osteogenic differentiation in hBMSCs. Those data suggested that *TAF1* was negatively related to the osteogenic differentiation of hBMSCs and disclosed the competitive endogenous RNA (ceRNA) network formed by *GAS5*/miR-382-3p/*TAF1*. Additionally, it was worth noting that *TAF1* can function as a transcription factor (36–38). Herein, we predicted that *TAF1* potentially bound to the *GAS5* promoter. Then, we validated the binding ability between them and discovered that *TAF1* could promote *GAS5* transcription. Those data suggested that *GAS5*/miR-382-3p/*TAF1* formed a positive feedback loop to inhibit the osteogenic differentiation of hBMSCs.

In conclusion, our study was the first to discover that *GAS5* (transcript variant 2) was downregulated in hBMSCs and could negatively regulate the osteogenic differentiation of hBMSCs. In addition, we revealed that *GAS5* could inhibit miR-382-3p via the TDMD mechanism to upregulate *TAF1*. Moreover, *TAF1* could bind to the *GAS5* promoter to activate its transcription so that a feed-forward loop of *GAS5*/miR-382-3p/*TAF1* could negatively regulate osteogenic differentiation.

There were also some limitations in our study, as it lacked *in vivo* experimental data. Therefore, we would carry out in *vivo* assays in our future study to directly validate the function of *GAS5* in osteogenesis. Nevertheless, our data uncovered the novel functions and mechanism of the *GAS5* variant and might provide new clues for mechanism research on the osteogenic differentiation of hBMSCs. In addition, *GAS5* was identified as a novel marker during the osteogenic differentiation of hBMSCs by our study.

**TABLE 1** Sequences of transfection plasmids

| Plasmid | Sequence (5′→3′) |
|---|---|
| sh-NC(for *GAS5*) | CCGGATCCTCTCTGTAGTCCTAGATCTCGAGATCTAGGACTACAGAGAGGATTTTTTG |
| sh-*GAS5*-1 | CCGGTGACATTTTGCCCTTTAGCCACTCGAGTGGCTAAAGGGCAAAATGTCATTTTTG |
| sh-*GAS5*-2 | CCGGAGTTTGAGGCTGTAGTAAGCTCTCGAGAGCTTACTACAGCCTCAAACTTTTTG |
| NC-mimics | cuauacgaugauccaacacau |
| miR-382-3p-mimics | aaucauucacggacaacacuu |
| NC-inhibitor | ugugauccguggauauauagu |
| miR-382-3p-inhibitor | aaguguuguccgugaaugauu |

## MATERIALS AND METHODS

**Cell culture.** Fluid was extracted from artificial hip joint replacements, and Ficoll-Hypaque density gradient centrifugation was performed for the extraction of human bone marrow mesenchymal stem cells (hBMSCs). Dulbecco's modified Eagle's medium (DMEM; HyClone, Logan, UT, USA) supplemented with 10% fetal bovine serum (FBS; Invitrogen, Waltham, MA, USA) was used for cell incubation at 37°C with 5% $CO_2$.

For osteogenic induction, hBMSCs were incubated with osteogenic medium (OM) containing growth medium (GM), 0.05 mmol/L ascorbate acid (Sigma, Merck KGaA, Darmstadt, Germany), 100 mmol/L dexamethasone (Sigma), and 10 mmol/L $\beta$-glycerophosphate (Sigma).

**Cell transfection.** When hBMSCs were growing well at passage 3, they were seeded into 6-well plates, which were supplied with complete medium. When confluence reached approximately 50%, the cells were processed with shRNAs targeting *GAS5* (sh-*GAS5*-1/2/3) or *TAF1* (sh-*TAF1*-1/2), pcDNA3.1/*GAS5*, miR-382-3p mimics, miR-382-3p inhibitor, and the corresponding negative controls (all synthesized by GenePharma, Shanghai, China) using Lipofectamine 2000 (Gibco, NE, USA) following the manufacturer's instructions.

**Total RNA extraction and RT-qPCR.** After osteogenic induction, total RNA was extracted from hBMSCs using TRIzol reagent (Invitrogen, CA, USA). Subsequently, reverse transcription (RT) of RNA into complementary DNAs (cDNAs) was carried out using PrimeScript RT reagent kit (TaKaRa, Dalian, China). Fluorescence quantitative PCR was then carried out in line with the guidebook of SYBR Premix Ex Taq II kit (TaKaRa) on the ABI Prism 7300 system (Applied Biosystems, CA, USA). Sequences of transfection plasmids are included in Table 1, and sequences for RT-qPCR probes and PCR primers are listed in Table S1 in the supplemental material.

**Western blot analysis.** Total protein was extracted via cell lysis using radioimmunoprecipitation assay buffer (DGCS Biotechnology, Beijing, China). Then, 10% sodium dodecyl sulfate polyacrylamide gel electrophoresis was utilized for the separation of the cell lysate. The isolated proteins were subsequently transferred onto a polyvinylidene fluoride membrane (Millipore, MA, USA), which was then blocked with 5% nonfat milk. After 2 h, the membrane was incubated with primary antibodies of *RUNX2* (1:1,000; Cell Signaling Technology, MA, USA), Osterix (*OSX*; 1:1,000; Abcam, Cambridge, UK), *TAF1* (1:1,000; Abcam), and GAPDH (glyceraldehyde-3-phosphate dehydrogenase; 1:1,000; Cell Signaling Technology). Afterward, the immune complexes were subjected to immunoblotting with an anti-mouse or anti-rabbit IgG (1:2,000; CWBio, Beijing, China). Enhanced chemiluminescence reagents (Fdbio, Hangzhou, China) were utilized for immunodetection.

**ChIP assay.** Following the protocol, an EZ ChIP chromatin immunoprecipitation kit (catalog no. 17-295) obtained from Millipore (Billerica, MA, USA) was applied to carry out the ChIP assay. Chromatin was cross-linked and sonicated to 200- to 1,000-bp fragments, followed by immunoprecipitation with anti-TAF1 (Abcam) or negative-control anti-IgG (Millipore, Billerica, MA, USA). The enrichment of DNA was quantified through RT-qPCR with GAPDH as the internal control.

**ALP staining.** After osteogenic induction, hBMSCs were subjected to 5 min of lysis and 3 min of centrifugation for acquiring supernatant. Then, 5 $\mu$L of supernatant supplemented with ALP substrate buffer (20 $\mu$L) was added to supernatant (5 $\mu$L). After mixture and a 1-h reaction, colorimetric analysis was employed for the detection of the ALP activity.

ALP staining (Gefan Biotechnology, Shanghai, China) was then used. Naphthol AS-MX phosphate (0.1 mg/mL) and Fast Blue BB salt (0.6 mg/mL) were used for ALP staining at room temperature in the darkness for 45 min. The results were observed and imaged under a light microscope.

**ARS staining.** ARS staining was employed for the measurement of mineralization. After being fixed by 4% paraformaldehyde for half an hour and washed with phosphate-buffered saline (PBS) twice, the cells were stained by 0.5% ARS staining solution at room temperature for 10 min. At last, the staining results were imaged.

**Dual-luciferase reporter assay.** The wild type (WT) and mutant type (Mut) containing the 3′ untranslated region (3′ UTR) of *TAF1* were synthesized and subcloned into pmirGLO reporters (Promega, WI, USA), and the Renilla luciferase served as an internal normalizer. The miR-382-3p mimics, miR-382-3p inhibitor, and the negative controls (NCs) were cotransfected with the luciferase reporter vector as required. The luciferase activity was examined following Promega's protocol.

**RIP assay.** In the RIP assay, an RNA binding protein immunoprecipitation kit obtained from Millipore was used following the manufacturer's instructions. Cells were lysed with RNA lysis buffer. Then, cell lysates were incubated with magnetic beads conjugated to anti-AGO2 (1:1,000; Abcam) or anti-IgG (the

negative control) at 4°C for 4 h. Next, the beads were washed, and the immunoprecipitated complex was purified and detected by RT-qPCR analysis.

**Statistical analysis.** Data analysis was performed using the SPSS 21.0 software (IBM, NY, USA). All data were exhibited as mean ± standard deviation (SD). Comparison between groups was conducted via *t* test, while differences among three or more groups were analyzed via one-way analysis of variance (one-way ANOVA). A $P$ value of $<0.05$ was set as the threshold of statistical significance.

## SUPPLEMENTAL MATERIAL

Supplemental material is available online only.

**SUPPLEMENTAL FILE 1**, PDF file, 0.1 MB.

## ACKNOWLEDGMENTS

We sincerely appreciate members who contributed to this study.

This study was supported by Lanzhou City Talent Innovation and Entrepreneurship Project (2019-RC-32).

We have no conflict of interest to declare.

## REFERENCES

1. Oryan A, Monazzah S, Bigham-Sadegh A. 2015. Bone injury and fracture healing biology. Biomed Environ Sci 28:57–71. https://doi.org/10.3967/bes2015.006.
2. Dimitriou R, Jones E, McGonagle D, Giannoudis PV. 2011. Bone regeneration: current concepts and future directions. BMC Med 9:66. https://doi.org/10.1186/1741-7015-9-66.
3. Liu H, Zhong L, Yuan T, Chen S, Zhou Y, An L, Guo Y, Fan M, Li Y, Sun Y, Li W, Shi Q, Weng Y. 2018. MicroRNA-155 inhibits the osteogenic differentiation of mesenchymal stem cells induced by BMP9 via downregulation of BMP signaling pathway. Int J Mol Med 41:3379–3393. https://doi.org/10.3892/ijmm.2018.3526.
4. Rumman M, Dhawan J, Kassem M. 2015. Concise review: quiescence in adult stem cells: biological significance and relevance to tissue regeneration. Stem Cells 33:2903–2912. https://doi.org/10.1002/stem.2056.
5. Xiao WZ, Gu XC, Hu B, Liu XW, Zi Y, Li M. 2016. Role of microRNA-129-5p in osteoblast differentiation from bone marrow mesenchymal stem cells. Cell Mol Biol (Noisy-le-grand) 62:95–99.
6. Ju C, Liu R, Zhang YW, Zhang Y, Zhou R, Sun J, Lv XB, Zhang Z. 2019. Mesenchymal stem cell-associated lncRNA in osteogenic differentiation. Biomed Pharmacother 115:108912. https://doi.org/10.1016/j.biopha.2019.108912.
7. Wang KC, Chang HY. 2011. Molecular mechanisms of long noncoding RNAs. Mol Cell 43:904–914. https://doi.org/10.1016/j.molcel.2011.08.018.
8. Zhang J, Tao Z, Wang Y. 2018. Long noncoding RNA DANCR regulates the proliferation and osteogenic differentiation of human bone-derived marrow mesenchymal stem cells via the p38 MAPK pathway. Int J Mol Med 41:213–219. https://doi.org/10.3892/ijmm.2017.3215.
9. Feng X, Lin T, Liu X, Yang C, Yang S, Fu D. 2018. Long non-coding RNA BDNF-AS modulates osteogenic differentiation of bone marrow-derived mesenchymal stem cells. Mol Cell Biochem 445:59–65. https://doi.org/10.1007/s11010-017-3251-2.
10. Wang Q, Li Y, Zhang Y, Ma L, Lin L, Meng J, Jiang L, Wang L, Zhou P, Zhang Y. 2017. LncRNA MEG3 inhibited osteogenic differentiation of bone marrow mesenchymal stem cells from postmenopausal osteoporosis by targeting miR-133a-3p. Biomed Pharmacother 89:1178–1186. https://doi.org/10.1016/j.biopha.2017.02.090.
11. Mourtada-Maarabouni M, Hedge VL, Kirkham L, Farzaneh F, Williams GT. 2008. Growth arrest in human T-cells is controlled by the non-coding RNA growth-arrest-specific transcript 5 (GAS5). J Cell Sci 121:939–946. https://doi.org/10.1242/jcs.024646.
12. Li M, Xie Z, Wang P, Li J, Liu W, Tang S, Liu Z, Wu X, Wu Y, Shen H. 2018. The long noncoding RNA GAS5 negatively regulates the adipogenic differentiation of MSCs by modulating the miR-18a/CTGF axis as a ceRNA. Cell Death Dis 9:554. https://doi.org/10.1038/s41419-018-0627-5.
13. Tu J, Tian G, Cheung HH, Wei W, Lee TL. 2018. Gas5 is an essential lncRNA regulator for self-renewal and pluripotency of mouse embryonic stem cells and induced pluripotent stem cells. Stem Cell Res Ther 9:71. https://doi.org/10.1186/s13287-018-0813-5.
14. Yang Q, Han Y, Liu P, Huang Y, Li X, Jia L, Zheng Y, Li W. 2020. Long noncoding RNA GAS5 promotes osteogenic differentiation of human periodontal ligament stem cells by regulating GDF5 and p38/JNK signaling pathway. Front Pharmacol 11:701. https://doi.org/10.3389/fphar.2020.00701.
15. Wang X, Zhao D, Zhu Y, Dong Y, Liu Y. 2019. Long non-coding RNA GAS5 promotes osteogenic differentiation of bone marrow mesenchymal stem cells by regulating the miR-135a-5p/FOXO1 pathway. Mol Cell Endocrinol 496:110534. https://doi.org/10.1016/j.mce.2019.110534.
16. Cho H, Li Y, Archacki S, Wang F, Yu G, Chakrabarti S, Guo Y, Chen Q, Wang QK. 2020. Splice variants of lncRNA RNA ANRIL exert opposing effects on endothelial cell activities associated with coronary artery disease. RNA Biol 17:1391–1401. https://doi.org/10.1080/15476286.2020.1771519.
17. Wu S, Nitschke K, Worst TS, Fierek A, Weis CA, Eckstein M, Porubsky S, Kriegmair M, Erben P. 2020. Long noncoding RNA MIR31HG and its splice variants regulate proliferation and migration: prognostic implications for muscle invasive bladder cancer. J Exp Clin Cancer Res 39:288. https://doi.org/10.1186/s13046-020-01795-5.
18. Bian X, Sun YM, Wang LM, Shang YL. 2021. ELK1-induced upregulation lncRNA LINC02381 accelerates the osteosarcoma tumorigenesis through targeting CDCA4 via sponging miR-503-5p. Biochem Biophys Res Commun 548:112–119. https://doi.org/10.1016/j.bbrc.2021.02.072.
19. Heilmeier U, Hackl M, Skalicky S, Weilner S, Schroeder F, Vierlinger K, Patsch JM, Baum T, Oberbauer E, Lobach I, Burghardt AJ, Schwartz AV, Grillari J, Link TM. 2016. Serum miRNA signatures are indicative of skeletal fractures in postmenopausal women with and without type 2 diabetes and influence osteogenic and adipogenic differentiation of adipose tissue-derived mesenchymal stem cells in vitro. J Bone Miner Res 31:2173–2192. https://doi.org/10.1002/jbmr.2897.
20. Libri V, Helwak A, Miesen P, Santhakumar D, Borger JG, Kudla G, Grey F, Tollervey D, Buck AH. 2012. Murine cytomegalovirus encodes a miR-27 inhibitor disguised as a target. Proc Natl Acad Sci U S A 109:279–284. https://doi.org/10.1073/pnas.1114204109.
21. Iwata J, Hosokawa R, Sanchez-Lara PA, Urata M, Slavkin H, Chai Y. 2010. Transforming growth factor-beta regulates basal transcriptional regulatory machinery to control cell proliferation and differentiation in cranial neural crest-derived osteoprogenitor cells. J Biol Chem 285:4975–4982. https://doi.org/10.1074/jbc.M109.035105.
22. Weinzierl RO, Dynlacht BD, Tjian R. 1993. Largest subunit of Drosophila transcription factor IID directs assembly of a complex containing TBP and a coactivator. Nature 362:511–517. https://doi.org/10.1038/362511a0.
23. Yu L, Gao Y, Ji B, Feng Z, Li T, Luan W. 2021. CTCF-induced upregulation of LINC01207 promotes gastric cancer progression via miR-1301-3p/PODXL axis. Dig Liver Dis 53:486–495. https://doi.org/10.1016/j.dld.2020.12.006.
24. Pu FF, Shi DY, Chen T, Liu YX, Zhong BL, Zhang ZC, Liu WJ, Wu Q, Wang BC, Shao ZW, He TC, Liu JX. 2021. SP1-induced long non-coding RNA SNHG6 facilitates the carcinogenesis of chondrosarcoma through inhibiting KLF6 by recruiting EZH2. Cell Death Dis 12:59. https://doi.org/10.1038/s41419-020-03352-6.
25. Jin C, Jia L, Huang Y, Zheng Y, Du N, Liu Y, Zhou Y. 2016. Inhibition of lncRNA MIR31HG promotes osteogenic differentiation of human adipose-

derived stem cells. Stem Cells 34:2707–2720. https://doi.org/10.1002/stem.2439.
26. Chen X, Yang L, Ge D, Wang W, Yin Z, Yan J, Cao X, Jiang C, Zheng S, Liang B. 2019. Long non-coding RNA XIST promotes osteoporosis through inhibiting bone marrow mesenchymal stem cell differentiation. Exp Ther Med 17:803–811. https://doi.org/10.3892/etm.2018.7033.
27. Peng W, Zhu SX, Wang J, Chen LL, Weng JQ, Chen SL. 2018. Lnc-NTF3-5 promotes osteogenic differentiation of maxillary sinus membrane stem cells via sponging miR-93-3p. Clin Implant Dent Relat Res 20:110–121. https://doi.org/10.1111/cid.12553.
28. Zheng D, Wang B, Zhu X, Hu J, Sun J, Xuan J, Ge Z. 2019. LncRNA OIP5-AS1 inhibits osteoblast differentiation of valve interstitial cells via miR-137/TWIST11 axis. Biochem Biophys Res Commun 511:826–832. https://doi.org/10.1016/j.bbrc.2019.02.109.
29. Coccia EM, Cicala C, Charlesworth A, Ciccarelli C, Rossi GB, Philipson L, Sorrentino V. 1992. Regulation and expression of a growth arrest-specific gene (gas5) during growth, differentiation, and development. Mol Cell Biol 12:3514–3521. https://doi.org/10.1128/mcb.12.8.3514-3521.1992.
30. Tang R, Zhang G, Wang YC, Mei X, Chen SY. 2017. The long non-coding RNA GAS5 regulates transforming growth factor beta (TGF-beta)-induced smooth muscle cell differentiation via RNA Smad-binding elements. J Biol Chem 292:14270–14278. https://doi.org/10.1074/jbc.M117.790030.
31. Li Y, Huo J, Pan X, Wang C, Ma X. 2018. MicroRNA 302b-3p/302c-3p/302d-3p inhibits epithelial-mesenchymal transition and promotes apoptosis in human endometrial carcinoma cells. Onco Targets Ther 11:1275–1284. https://doi.org/10.2147/OTT.S154517.
32. Tao W, Ma J, Zheng J, Liu X, Liu Y, Ruan X, Shen S, Shao L, Chen J, Xue Y. 2020. Silencing SCAMP1-TV2 inhibited the malignant biological behaviors of breast cancer cells by interaction with PUM2 to facilitate INSM1 mRNA degradation. Front Oncol 10:613. https://doi.org/10.3389/fonc.2020.00613.
33. Chang X, Zhang H, Yang Q, Pang L. 2020. LncRNA SOX2OT affects cervical cancer cell growth, migration and invasion by regulating SOX2. Cell Cycle 19:1391–1403. https://doi.org/10.1080/15384101.2020.1750812.
34. Che M, Gong W, Zhao Y, Liu M. 2020. Long noncoding RNA HCG18 inhibits the differentiation of human bone marrow-derived mesenchymal stem cells in osteoporosis by targeting miR-30a-5p/NOTCH1 axis. Mol Med 26:106. https://doi.org/10.1186/s10020-020-00219-6.
35. Xiang J, Fu HQ, Xu Z, Fan WJ, Liu F, Chen B. 2020. lncRNA SNHG1 attenuates osteogenic differentiation via the miR-101/DKK1 axis in bone marrow mesenchymal stem cells. Mol Med Rep 22:3715–3722. https://doi.org/10.3892/mmr.2020.11489.
36. Maile T, Kwoczynski S, Katzenberger RJ, Wassarman DA, Sauer F. 2004. TAF1 activates transcription by phosphorylation of serine 33 in histone H2B. Science 304:1010–1014. https://doi.org/10.1126/science.1095001.
37. Tavassoli P, Wafa LA, Cheng H, Zoubeidi A, Fazli L, Gleave M, Snoek R, Rennie PS. 2010. TAF1 differentially enhances androgen receptor transcriptional activity via its N-terminal kinase and ubiquitin-activating and -conjugating domains. Mol Endocrinol 24:696–708. https://doi.org/10.1210/me.2009-0229.
38. Thomas MC, Chiang CM. 2006. The general transcription machinery and general cofactors. Crit Rev Biochem Mol Biol 41:105–178. https://doi.org/10.1080/10409230600648736.